Carbohydrate Research, 160 (1987) 369–380
Elsevier Science Publishers B.V., Amsterdam – Printed in The Netherlands

STRUCTURAL AND RHEOLOGICAL INVESTIGATIONS ON THE LYOTROPIC, LIQUID-CRYSTALLINE SYSTEM: *O*-ETHYLCELLULOSE–ACETIC ACID–DICHLOROACETIC ACID

PETER ZUGENMAIER AND PETRA HAURAND

Institut für Physikalische Chemie der TU Clausthal, D-3392 Clausthal-Zellerfeld (Federal Republic of Germany)

(Received March 28th, 1986, accepted for publication in revised form, July 11th, 1986)

ABSTRACT

The lyotropic, cholesteric system consisting of *O*-ethylcellulose–acetic acid–dichloroacetic acid was investigated in the whole mixing range with respect to structural features and flow behavior. The cholesteric helicoidal structure varies in this system from a left- to a right-handed twist with increasing volume fraction of dichloroacetic acid, and the twist angle becomes zero at a certain mixing ratio, resulting in a quasi-nematic phase. The pitch of the helicoidal structure was determined by optical rotatory dispersion and transmission spectra, and correlated to the viscosity measured in a concentric-cylinder, rotational viscosimeter. High shear-thinning was observed for the quasi-nematic phase, and explained by a model proposed by Onogi and Asada. The phase behavior was characterized by a thermomicroscopic study, and the birefringence was determined on surface-aligned samples by means of an Abbé refractometer.

INTRODUCTION

It has been known for a decade that cellulose derivatives form lyotropic, cholesteric, liquid-crystalline phases[1]. De Vries[2] basically treated cholesteric phases in a theoretical study, and proposed useful equations that connect structural features with optical properties, and provide explanations of unusual optical properties of these systems. The model for his considerations consists of twisted, nematic sheets with a left- or right-handed twisting-angle, resulting in a helicoidal structure with a certain pitch.

In the present investigation[3], our interest was focussed on a special cellulose derivative–solvent system. It was observed[4] that *O*-ethylcellulose (EC) in acetic acid (HOAc) forms a lyotropic, cholesteric structure with left-handed twisting-angle and, in contrast, EC in dichloroacetic acid ($CHCl_2CO_2H$), a cholesteric structure with right-handed twisting-angle. A mixture of the two solvents in a certain ratio should cancel the twisting power, and a metastable "nematic" phase should exist with a pitch, of size infinity, that is called a quasi-nematic phase. A change of the

0008-6215/87/$ 03 50

flow behavior is to be expected when the cholesteric system passes through this structural transition. Therefore, the goal of this study was a careful, structural characterization of the cholesteric phases of EC–acetic acid–dichloroacetic acid, and a correlation of these data to the flow behavior

EXPERIMENTAL

Commercially available *O*-ethylcellulose (EC; Fluka AG, characterized by 45 mPa.s for a concentration of 5% at 25°; degree of substitution ~2.5) was used throughout this study. A series of 11 EC–acetic acid–dichloroacetic acid samples of 0.8 g/mL (EC–mixed solvent) was prepared by changing the amount of $CHCl_2CO_2H$ in steps of 10 vol-%, starting with 0.8 g of EC dissolved in 1 mL of pure HOAc and covering the whole range from 0 to 100 vol-% $CHCl_2CO_2H$ in HOAc. Exactly 8 days after preparation, the samples were placed in different measuring devices to ensure proper dissolution, precise experimental conditions, and, for each system, equal changes on the EC molecule, such as degradation and substitution of the OH groups still available. Some of the samples show the typical, irridescent colors of cholesteric phases. The reflection colors observed perpendicular to the surface of aligned samples range from dark blue, for EC in pure HOAc, to turquoise, yellow, orange, and red for the samples with increasing amounts of $CHCl_2CO_2H$ in steps of 10 vol-%.

The wavelength of light reflected from samples having more than 50 vol-% $CHCl_2CO_2H$ is outside the visible range. Structural details of the cholesteric phases as the pitch p of the helicoidal structure can be determined by knowledge of the optical rotatory power θ or transmission spectra, and the cholesteric refractive indices. Such measurements were performed on surface-aligned samples that were produced by rubbing the covering glass plates of the samples with a cloth in one direction. A detailed description of the determination of the pitch, and a discussion of the validity of these methods is given in previous reports[5,6] for some selected cellulose derivative–solvent systems, and uses as its basis the theory of de Vries[2].

Cholesteric phases attenuate light at a certain wavelength λ_0 by a selective reflection. This wavelength is related to the pitch p by

$$\lambda_0 = \bar{n}\, p, \tag{1}$$

with $\bar{n}$ the mean refractive index of a nematic plane that can be related to the actual, measured cholesteric ordinary and extraordinary refractive index, $n_{o,ch}$ and $n_{e,ch}$, respectively[5,6]. The wavelength of selective reflection λ_0 is determined by the minimum of the transmission spectra, or by the optical rotatory spectra curves.

The optical rotatory power θ is a function of the wavelength λ used in the experiment[2]:

$$\theta = \frac{\pi}{4} \frac{\Delta n_n^2}{\lambda^2} \cdot \frac{p}{1 - (\lambda/\lambda_0)^2}, \tag{2}$$

with a positive sign of p for a right-handed, and a negative one for a left-handed, helicoidal, cholesteric structure.

The nematic birefringence Δn_n is given by

$$\Delta n_n = -2\, \Delta n_{ch}, \tag{3}$$

Δn_{ch} being the cholesteric birefringence, with sufficient accuracy for cellulose derivative–solvent systems[5].

Fig. 1 depicts a schematic diagram for the relationship $\theta(\lambda)$ according to Eq. *2* for positive p. Two singularities are found, one for $\lambda = \lambda_0$, the other for $\lambda = 0$, and a minimum at $\lambda_{min} = \lambda_0/\sqrt{2}$. The pitch p can be determined with Eq. *1*, with λ_0 known (*i*) through the singularity $\lambda = \lambda_0$, which means that θ becomes zero for experimentally determined curves at that point, or (*ii*) through the knowledge of λ_{min}, from which λ_0 can also be obtained. An evaluation of Eq. *2* with $\lambda/\lambda_0 \ll 1$ results in

$$\theta = \frac{\pi}{4} \cdot \Delta n_n^2 \cdot p \cdot \frac{1}{\lambda^2}. \tag{2'}$$

The slope of a plot of θ *versus* λ^{-2} determines p with Δn_n known.

A mirror image of the curve at $\theta = 0$ in Fig. 1 is obtained for $p < 0$ with a maximum $\lambda_{max} = \lambda_0/\sqrt{2}$. The sign of θ for $\lambda < \lambda_0$ determines the handedness of the helicoidal, cholesteric structure, with $\theta > 0$ for a right-handed twist, and $\theta < 0$ for a left-handed one.

The optical rotatory power was measured on surface-aligned samples, 36 μm

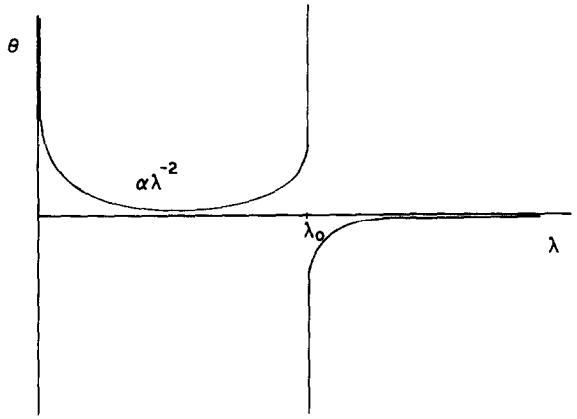

Fig 1. Schematic representation of Eq. *2* with $p > 0$

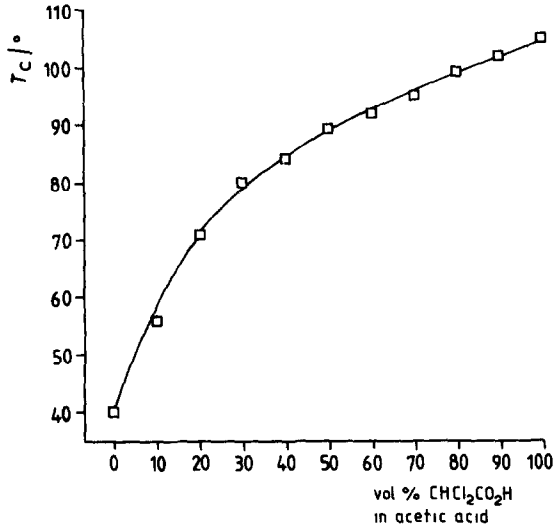

Fig 2 Clearing temperature T_c *versus* vol-% $CHCl_2CO_2H$ in HOAc for lyotropic, liquid-crystalline *O*-ethyl-cellulose

thick, with a Perkin–Elmer 241 MC instrument in the wavelength range 380–600 nm. The transmission spectra were recorded in the u.v.-v.i.s.-n.i.r. range with a Perkin–Elmer instrument. The sample preparation was the same as for optical rotatory power measurements.

The phase diagram of Fig. 2 (clearing temperature T_c *versus* vol-% $CHCl_2CO_2H$) was obtained by analyzing the textures with a polarizing microscope (Olympus BH-2) having a heating stage (Mettler FP5/FP52).

RESULTS•

Phase behavior. — Polarizing-microscope studies of surface-aligned samples reveal a decrease of orientation with increasing amount of $CHCl_2CO_2H$ in the orthoscopic and conoscopic observation mode. This observation may be due to an increase of viscosity, to be discussed later, that reduces the mobility of the phase.

A two-phase system is observed just below the clearing temperature (*cf.*, Fig. 2) for samples with 50 vol-% $CHCl_2CO_2H$ and more. A similar phase-separation behavior was found on polyisocyanate systems at room temperature as a function of time[7]. According to Flory[8], the concentrated solution is separated into an isotropic phase with a low molecular-mass fraction of polymeric material and an ordered anisotropic phase with a higher molecular-mass fraction of higher concentration.

Growth of spherulites and crystals occurs for samples with >50 vol-% $CHCl_2CO_2H$ when the samples are cooled from the clearing temperature to room temperature The size of the spherulites increases with higher cooling rates. The

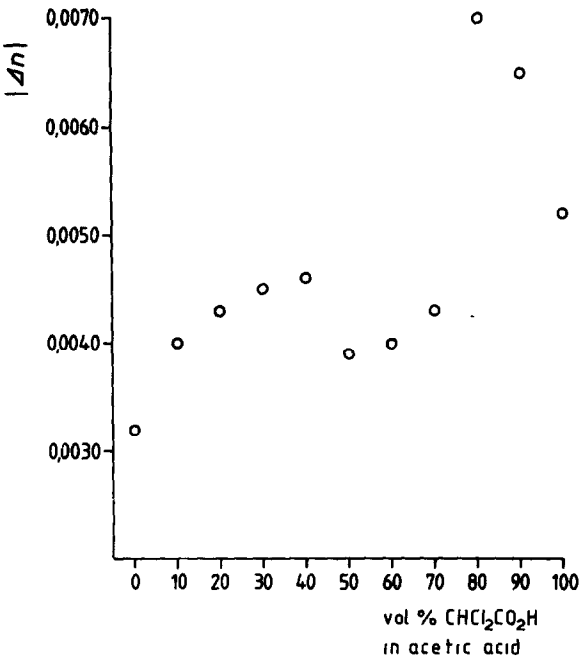

Fig 3. Representation of birefringence Δn_{ch} as a function of volume fraction $CHCl_2CO_2H$ at room temperature for liquid-crystalline EC

spherulites do not show the typical extinction patterns when observed between crossed polars, which agrees with the findings of Keith and Padden[9] for fast crystallization. The absence of the maltese cross is an indication of faulty orientation of the spherulites. The spherulites have a negative birefringence as the liquid crystalline phases, which will be discussed in the following section.

Birefringence. — The ordinary and extraordinary refractive indices were determined in an Abbé refractometer at room temperature (wavelength 589 nm). The very small birefringence $\Delta n_{ch} = n_{e,ch} - n_{o,ch}$ is negative, and is summarized in Fig. 3. Discontinuities at least appear at 50 and 80 vol-% $CHCl_2CO_2H$. The mean refractive indices almost linearly increase, with the small discontinuities scarcely visible, from 1.420 to 1.478 from 0 to 100 vol-% $CHCl_2CO_2H$.

Structural investigations. —The optical rotatory spectra for most of the 11 samples are presented in Figs. 4a, b. The wavelength λ_0 of zero value of optical rotatory power θ in Fig. 4a increases with increasing volume fraction of $CHCl_2CO_2H$ and agrees well with the minima of the transmission spectra. These wavelengths are in accord with the reflection colors described in the Experimental section. The pitch of the left-handed, helicoidal, cholesteric structure ($\theta < 0$ for $\lambda < \lambda_0$) is easily determined with Eq. *1*, as λ_0 and $\bar{n}$ are known.

The wavelength λ_0 of zero value of θ cannot be measured in Fig. 4b. The pitch is then determined with Eq. *2'* from a plot of $\theta(\lambda^{-2})$, or by the maximum of

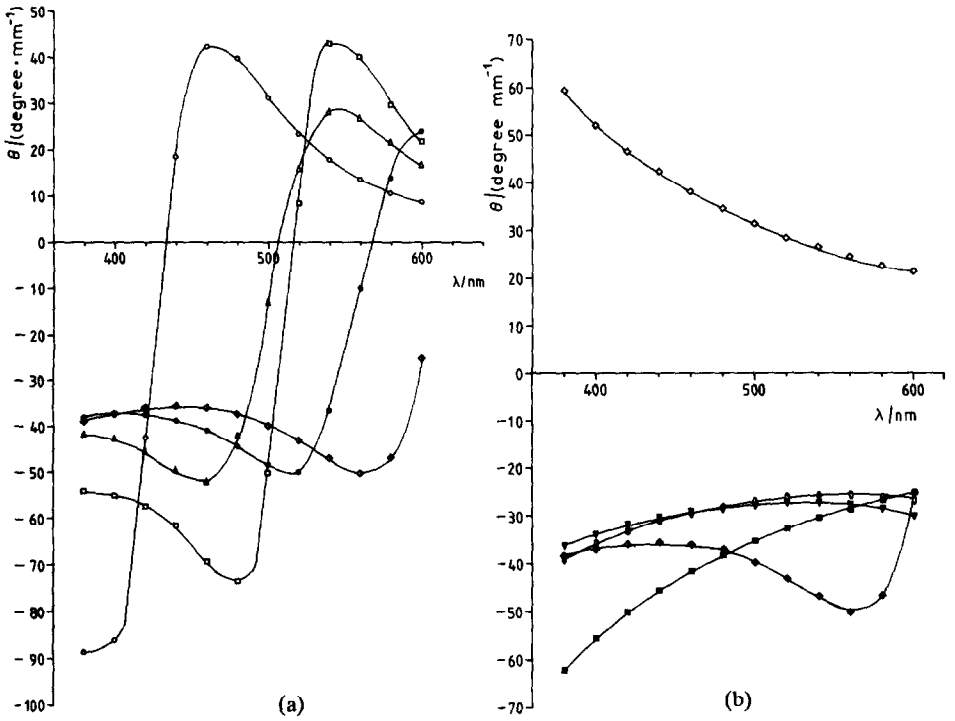

Fig 4 (a) Optical rotatory spectra for different volume fractions $CHCl_2CO_2H$ at room temperature for liquid-crystalline EC [Key· ○○, 0 vol-%; △△, 10 vol-%; □□, 20 vol-%, ●●, 30 vol-%, and ◆◆, 40 vol-%.] (b) Optical rotatory spectra for different volume fractions $CHCl_2CO_2H$ at room temperature for liquid-crystalline EC. [Key. ◆◆, 40 vol-%, ▼▼, 50 vol-%, ○○, 60 vol-%; ■■, 70 vol-%, and ◇◇, 100 vol-%]

the optical rotatory power curve through $\lambda_{max} = \lambda_0/\sqrt{2}$ with Eq. *1*, as shown in Fig. 5 for EC with 40 vol-% $CHCl_2CO_2H$. A comparison with the extrapolated λ_0 and the minimum of the transmission curve proves the correctness of the method. The pitch of samples with 80 and 90 vol-% $CHCl_2CO_2H$ are too large to be measured by optical rotatory or transmission spectra. The textures observed for these samples are of the cholesteric type. EC in pure $CHCl_2CO_2H$ gives an optical rotatory power curve with θ positive in the accessible range that can be evaluated according to Eq. *2'*. The cholesteric, helicoidal structure is right-handed, as θ is positive for $\lambda < \lambda_0$.

The results of the structural investigation are collected in Fig. 6, where the pitch p is plotted *versus* the volume fraction of $CHCl_2CO_2H$ for liquid-crystalline EC. The absolute value of the pitch of the left-handed, helicoidal structure increases with increasing volume fraction of $CHCl_2CO_2H$, and is −2750 nm for 70 vol-% $CHCl_2CO_2H$.

A positive value for the pitch that corresponds to a right-handed helicoidal structure is detected for EC in pure $CHCl_2CO_2H$ with p = 1870 nm. The accuracy for the determination of the pitch is much lower when Eq. *2'* is used, because the

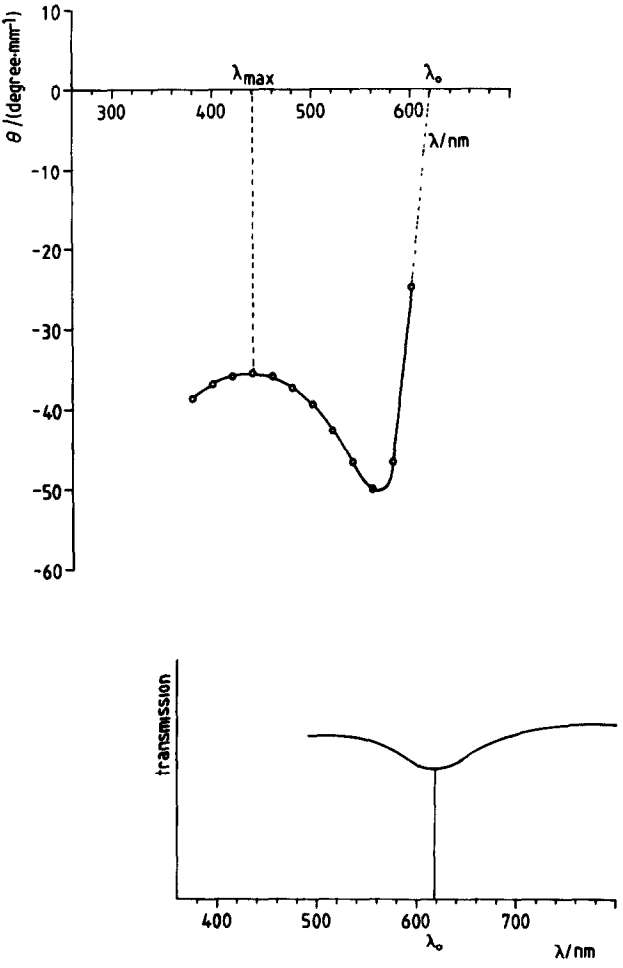

Fig 5. Comparison between λ_0 determined by optical rotatory and transmission spectra for liquid-crystalline EC with 40 vol-% $CHCl_2CO_2H$

necessary measurement of the birefrigence bears some uncertainty for such small values as are observed in EC–HOAc–$CHCl_2CO_2H$ systems.

Fig. 6 clearly shows a range in which the pitch tends to reach very large values and cannot be measured with currently available techniques. In this range, a structural transition occurs from a left-handed to a right-handed helicoidal structure that is the prerequisite for a quasi-nematic phase with twisting-angle zero.

Flow behavior. — Flow curves and the temperature dependence of viscosity were investigated as a function of volume fraction of $CHCl_2CO_2H$ in a solvent mixture with HOAc for liquid-crystalline *O*-ethylcellulose (EC).

The rheological study was carried out with a concentric-cylinder, rotational viscosimeter (Rheomat 30 of Contraves). A typical flow curve is presented in Fig.

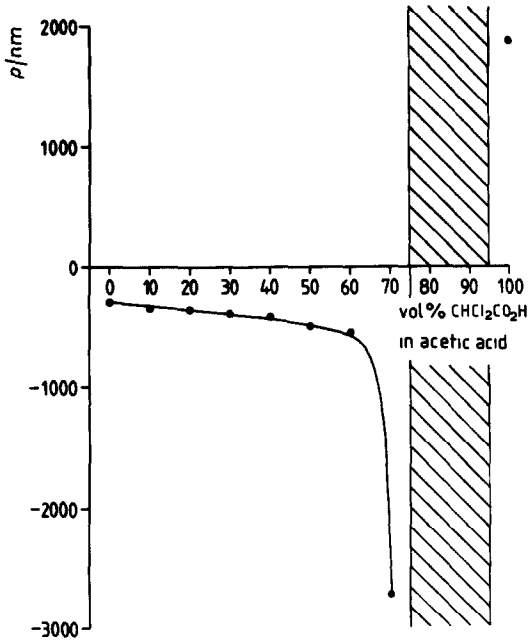

Fig. 6 Pitch p as a function of volume fraction $CHCl_2CO_2H$ for liquid-crystalline EC–HOAc–$CHCl_2CO_2H$

7 for a sample EC–HOAc (0 vol-% $CHCl_2CO_2H$) in a plot of log η *versus* log $\dot{\gamma}$ with η viscosity and $\dot{\gamma}$ shear rate. The flow curve is composed of three parts, each of which is a straight line. An interpretation of flow curves from lyotropic, cholesteric, liquid-crystalline systems consisting of three parts was given by Onogi and Asada[10].

Flow curves similar to those in Fig. 7 were recorded for higher volume fractions of $CHCl_2CO_2H$ for which, in some cases, the straight line at high shear-

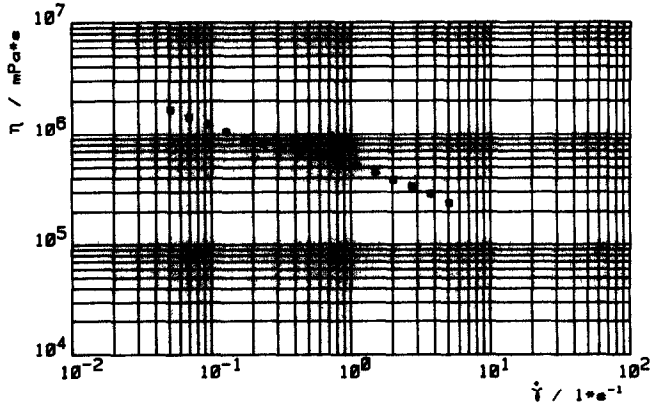

Fig 7. Flow curve for liquid-crystalline EC–HOAc (0 vol-% $CHCl_2CO_2H$) in a plot of log η *versus* log $\dot{\gamma}$ at 23°

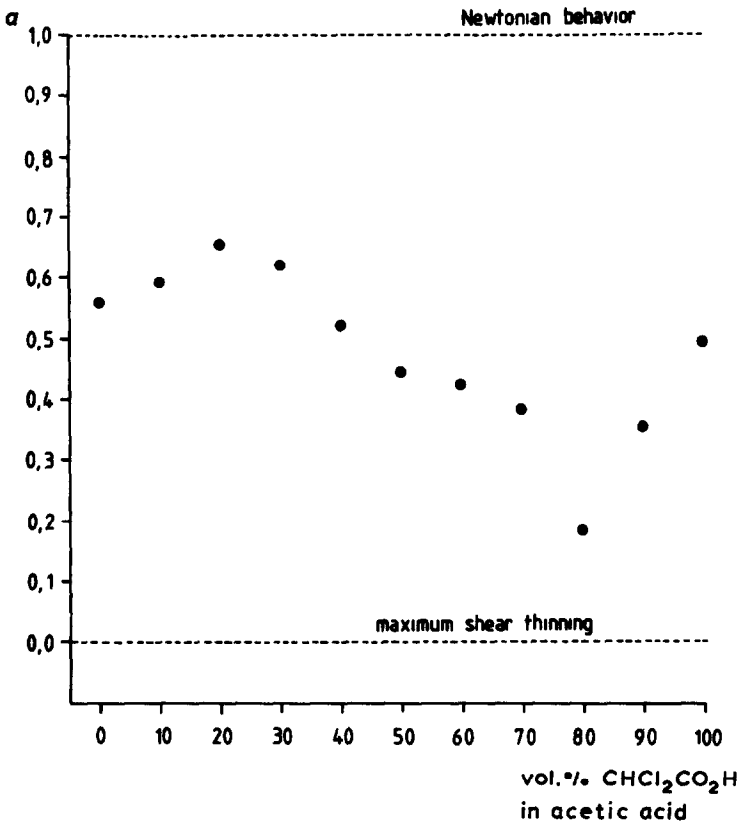

Fig 8. Exponent a of Eq. 5 as a function of volume fraction of $CHCl_2CO_2H$ for liquid-crystalline EC

rate, or the last two straight lines at high shear-rates, were missing. Only the first part of the flow curves at low shear-rates has been evaluated according to

$$\log \eta = \log C + (a - 1) \log \dot{\gamma}, \tag{4}$$

with C a constant and the value of a a measure for shear thinning. According to Onogi and Asada[10], this part of the flow curve represents a decomposition of almost all cholesteric domains, and an orientation of the molecules in the direction of flow which should occur at lower shear-stress τ for a quasi-nematic phase with all molecules already preoriented. The influence on a can be discussed with use of Eq. 5, which relates the shear stress τ to the shear rate for non-Newtonian flow behavior.

$$\tau = C \cdot \dot{\gamma}^a \tag{5}$$

A low value of a is to be expected for a quasi-nematic phase.

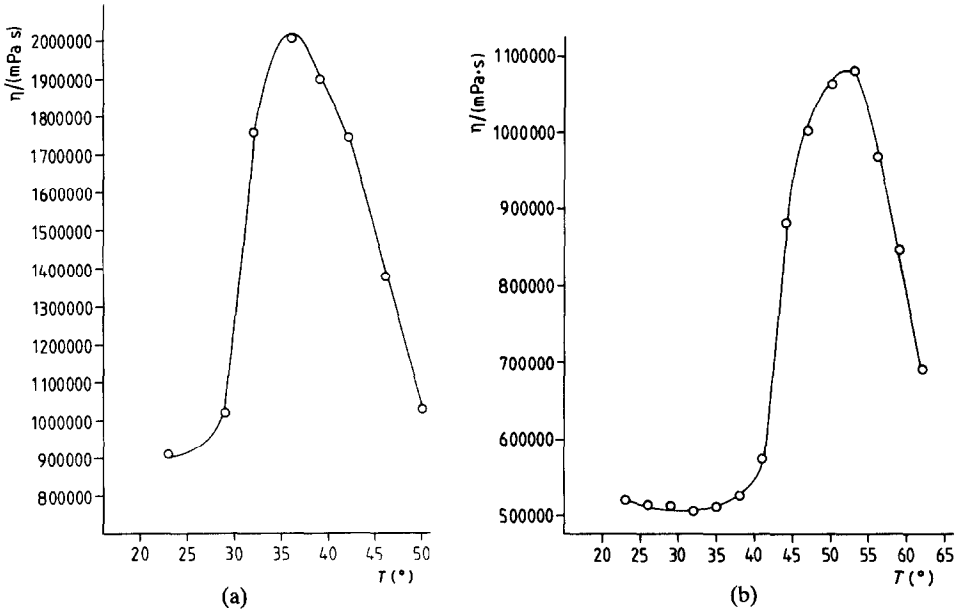

Fig 9 (a) Viscosity η as a function of temperature T for EC in HOAc (0 vol-% $CHCl_2CO_2H$) at a shear rate of 0 18 s^{-1} (b) Viscosity η as a function of temperature T for EC in HOAc-$CHCl_2CO_2H$ (10 vol-% $CHCl_2CO_2H$) at a shear rate of 0 18 s^{-1}

The result of the evaluation of the flow curves according to Eq. *4* is shown in Fig. 8 for liquid-crystalline EC with different volume fractions of $CHCl_2CO_2H$. This Figure clearly shows a very low value of $a = 0.18$ for a sample with 80 vol-% $CHCl_2CO_2H$ in the range of the expected quasi-nematic phase (according to Fig. 6).

The temperature-dependence of viscosity at low shear-rate ($\gamma = 0.18\ s^{-1}$) is presented in Figs. 9a,b for two samples when the cholesteric–isotropic phase-transition is passed from lower to higher temperatures. The maximum of both curves lies at temperatures 4° lower than the phase-transitions determined by thermomicroscopic investigations (see Fig 2). Due to experimental limitations, the samples with larger $CHCl_2CO_2H$ content, that is, higher clearing temperatures (see Fig. 2), could not be investigated. A drop of viscosity by a factor of almost two is observed at equivalent points (see Figs. 9a,b) when only ~10 vol-% $CHCl_2CO_2H$ is added to EC in pure HOAc.

In Fig. 10, the viscosity dependence at 23° is plotted as a function of volume fraction of $CHCl_2CO_2H$ at different shear-rates. The viscosity of EC in pure HOAc differs from that of EC in pure $CHCl_2CO_2H$ by a factor of 30, and reflects the increasing clearing-temperature with increasing volume fraction of $CHCl_2CO_2H$. In Fig. 10, the viscosity reaches a minimum at 20 vol-% $CHCl_2CO_2H$, and visibly changes its behavior at 50 vol-% for low shear-rates. The enormous drop of viscos-

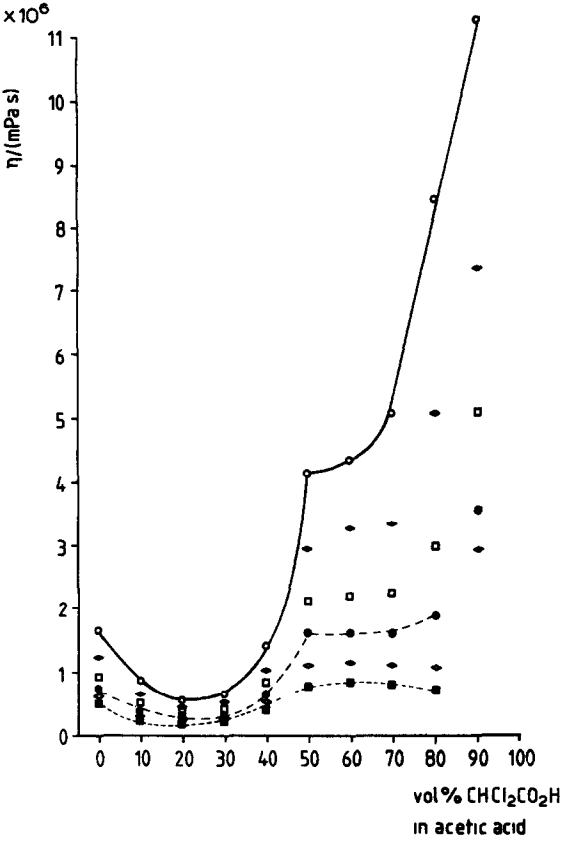

Fig 10 Viscosity η as a function of volume fraction of $CHCl_2CO_2H$ for liquid crystalline EC/HOAc-$CHCl_2CO_2H$ at different shear rates γ (temperature 23°). ○○, 0 05 s^{-1}; ◆◆, 0 09 s^{-1}, □□, 0.17 s^{-1}; ●●, 0 32 s^{-1}, ◇◇, 0 59 s^{-1}; ■■, 1 09 s^{-1}

ity is remarkable at larger shear-rates at higher-volume fractions of $CHCl_2CO_2H$. The viscosity remains in the order of magnitude of EC in pure HOAc up to 80 vol-% $CHCl_2CO_2H$.

DISCUSSION AND CONCLUSIONS

The flow behavior of the cholesteric, liquid-crystalline system EC–HOAc–$CHCl_2CO_2H$ is influenced by the internal structure of these phases. The presence of a quasi-nematic phase between 80 and 90 vol-% $CHCl_2CO_2H$ is reflected as a minimum for *a*, the power-law exponent in Eq. *5*, and a considerable drop of viscosity to higher shear-rates (see Fig. 10). The maximum of *a* at 20 vol-% $CHCl_2CO_2H$ in Fig. 8 corresponds to a minimum of viscosity in Fig. 10, and the discontinuity of the viscosity in Fig. 10 at 50 vol-% $CHCl_2CO_2H$ can be correlated to the appearance of a two-phase region (cholesteric–isotropic) at the phase transition in the thermomicroscopic studies, and a discontinuity of the birefringence in Fig. 3.

The quasi-nematic phase also evokes a large birefringence that is almost twice the value for cholesteric phases at small pitches (see Fig. 3), and compares to the ratio of the birefringence of a nematic sheet to the cholesteric, helicoidal structure. However, the optical axes are the same for the quasi-nematic and the cholesteric phases, as are the surface alignments.

In this investigation, it was shown that the change of viscosity with temperature can also be used for establishing phase diagrams, besides the detection of the phase transition, cholesteric–isotropic, in the usual manner, by thermomicroscopic observations of disappearance of textures under the polarizing microscope, or the disappearance of birefringence, *etc.* The maximum of viscosity as a function of temperature is ~4° lower than the phase transition determined by thermomicroscopy. The change of viscosity from the maximum of Fig. 9a to the minimum in the cholesteric phase is about a factor of two, and approximately reaches the drop, as by adding 10 vol-% $CHCl_2CO_2H$ to the system at the temperature of maximum viscosity. The viscosity can then be lowered by the same factor again, when this system is brought into the cholesteric phase.

It is clear that degradation of *O*-ethylcellulose occurs during sample preparation, and a broad molecular-mass distribution is present. An optical investigation on surface-aligned samples has been performed in the conoscopic-observation mode through the polarizing microscope, and biaxial optical behavior has been detected. At present, it seems that this optical behavior is caused by slightly different orientations of domains. Further studies are necessary for a better understanding of structural features, including the orientation parameter, the phase, and optical behavior of lyotropic, liquid-crystalline, cellulose-derivative systems.

REFERENCES

1 R. S. WERBOWYJ AND D. G. GRAY, *Mol. Cryst Liq Cryst. Lett.*, 34 (1976) 97–103; D. G. GRAY, *Current Topics on Cellulose and its Derivatives, Proc Daicel Cellulose Conf*, Aug 26–27, 1985, Himeji, Japan, pp. 83–97.
2 H. DE VRIES, *Acta Crystallogr.*, 4 (1951) 219–226.
3 P. HAURAND, Diplomarbeit, Institut fur Physikalische Chemie der TU Clausthal, D-3392 Clausthal-Zellerfeld, 1985.
4 U. VOGT, Dissertation, Institut fur Physikalische Chemie der TU Clausthal, D-3392 Clausthal-Zellerfeld, 1985
5 U VOGT AND P. ZUGENMAIER, *Makromol. Chem , Rapid Commun* , 4 (1983) 759–765.
6 U VOGT AND P ZUGENMAIER, *Ber Bunsenges. Phys Chem* , 89 (1985) 1217–1224
7 S M. AHARONI AND E. K. WALSH, *Macromolecules,* 12 (1979) 271–276
8 P J. FLORY, *Ber. Bunsenges. Phys. Chem.*, 81 (1977) 885–891
9 H D KEITH AND F J. PADDEN, JR , *J. Polym. Sci.*, 39 (1959) 101–137.
10 S ONOGI AND T ASADA, *Rheology,* 1 (1980) 127–146